JOURNAL OF CATALYSIS 152, 137–146 (1995)

Chain Length Dependence of α-Olefin Readsorption in Fischer–Tropsch Synthesis

E. W. Kuipers, I. H. Vinkenburg, and H. Oosterbeek

Koninklijke/Shell Laboratorium Amsterdam, P.O. Box 38000, 1030 BN Amsterdam, The Netherlands

Received May 16, 1994; revised August 12, 1994

The total product concentration and the paraffin/olefin ratio have been measured up to C_{14} for Fischer–Tropsch synthesis on polycrystalline Co foils. The influences due to surface area, a wax coating, the H_2/CO ratio and flow velocity on concentration and selectivity have been determined. The paraffin/olefin ratio increases exponentially with chain length which is attributed to a chain-length-dependent olefin readsorption mechanism. The probability of readsorption depends on the heat of physisorption of the olefins on the catalyst as well as on their heat of dissolution in and their diffusivity through the product wax. All three factors predict an increase of the paraffin/olefin ratio with carbon number. Physisorption and dissolution are shown to cause a much stronger chain-length dependence than diffusion and will usually dominate. © 1995 Academic Press, Inc.

INTRODUCTION

The ratio of established world gas reserves over established world oil reserves has increased almost threefold over the last two decades. This trend is expected to continue and will probably result in a shift towards gas as an important feedstock for transportation fuels (1). Transportation fuel can be manufactured by the initial conversion of methane to synthesis gas (CO/H_2) which is subsequently converted to linear hydrocarbons in the Fischer–Tropsch (FT) process. This process is a heterogeneously catalyzed reaction which yields a range of products primarily consisting of olefins, paraffins, and oxygenates (2, 3). Since FT is a polymerization reaction, its product yield decreases exponentially with chain length, a dependence usually referred to as the Anderson–Schulz–Flory (ASF) distribution. However, deviations from this ASF distribution are observed, usually as a higher-than-expected yield of longer hydrocarbons. During the last decade there has been considerable controversy about the cause of this deviation. Several different explanations have been proposed. At first it was suggested that in many cases it might only be an experimental artifact, since the deviation starts to occur in the chain length range where the products leaving the reactor become liquid (4). It soon became clear that the above ASF for C_{10+} yield was not an artifact at all and it was believed to be caused by two different catalytic sites yielding different chain growth probabilities (α's) (5, 6) since the product distributions could often be fitted by a superposition of two ASF distributions (7).

A more plausible cause for the deviation, however, is the occurrence of secondary reactions. Growing surface chains can terminate as paraffins or olefins, of which the latter can readsorb at the surface of the catalyst and again take part in the polymerisation reaction (2, 8). Readsorption reverses the termination, causing an increase in the net chain growth probability (9, 10). Hence the observed double ASF behaviour can also be explained by assuming a reinsertion probability that strongly increases with chain length, as has clearly been shown by Iglesia and co-workers (10–13). A negligible amount of the short α-olefins would then be readsorbed, whereas practically all the long α-olefins will be readsorbed. This results in a net chain growth probability which is higher for high carbon numbers, causing a larger C_{10+} selectivity than that predicted by ASF. It is generally assumed that the α-olefin readsorption chance increases with contact time inside the pores of the catalyst. Two different causes for a chain-length-dependent contact time have been proposed, namely a chain-length-dependent solubility in FT wax (14, 15) and a chain-length-dependent transport limitation (10–13). To obtain more insight into the chain-length dependence of the α-olefin readsorption rate, experiments on Co foil have been performed.

EXPERIMENTAL

The catalytic experiments were performed in a glass reactor as shown in Fig. 1. The reactor consists of two parts, which closely fit into one another and are suspended in an oven. This reactor design has the seals outside the heating zone and thus Viton "O"-rings can be used. Although the inside of the inner beaker is filled with glass wool for thermal insulation, there will still be a minor

0021-9517/95 $6.00

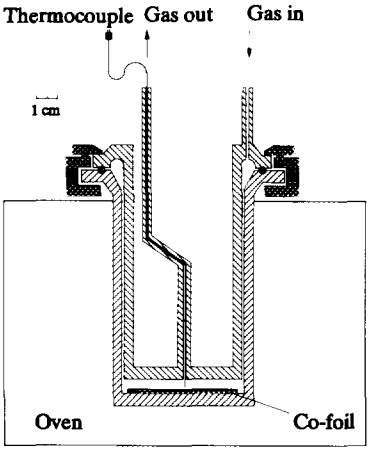

FIG. 1. Schematic representation of the glass reactor used.

temperature gradient in the reactor causing sufficient "stirring" due to convection in order to warrant continuous ideally stirred tank reactor (CISTR) behaviour. The temperature of the sample is measured by a Chromel/Alumel thermocouple. The reactor is operated in flow mode at 1 bar total pressure. The total reactor volume is 10 cm^3. Both a quadrupole mass spectrometer (QMS) and a gas chromatograph (GC) (Chrompack 9001) are attached to analyse the composition of the gas leaving the reactor. The GC separation of C_1 to C_5 is done on a Poraplot Q column and C_6 to C_{14} are separated on a CP-Sil-5 column. Flame ionisation detectors (FID) are used because of their high detection efficiency and linear response. All hydrocarbons and oxygenates up to C_{14} can be eluted. CO, CO_2, O_2, H_2O, and H_2 are monitored by the QMS. To prevent condensation of products, the tubes downstream are heated. Synthesis gas is prepared by mixing H_2 and CO via mass flow controllers, enabling any H_2/CO ratio to be obtained. Under standard reaction conditions (1 bar, 493 K, H_2/CO = 2) the activity of the empty reactor was too low to be detected. Polycrystalline cobalt foils (Goodfellow, purity 99.99%, thickness 0.25 mm) were used as a catalyst. The as-received foils were first reduced for 7 h under flowing H_2 at 673 K. Prior to every experiment the Co foils were calcined in air at 673–723 K for 4 h. The Co foils were subsequently reduced in a H_2 flow (10 Nml/min) at 1 bar and 573 K for several minutes. The paraffin selectivity is dependent on the reduction time. During the reduction the production of H_2O was monitored by the QMS. After reduction the H_2 flow was replaced by a flow of synthesis gas and reaction was carried out at 493 K. During all experiments conversions were very low (<1%) with the concentration of the CH_4 produced being around 1500 molecules per million gas molecules leaving the reactor, i.e., 1500 ppm. Standard reaction conditions gave a CO turnover-number of around $3.10^{13}/cm^2$ s, and a chain growth probability of 0.45 ± 0.02, both comparable to values previously reported for polycrystalline Co and a stepped Co single crystal surface (16, 17).

In some experiments C_{60+} FT wax (Shell) or Santovac 5 (Monsanto) (hexaphenyl-dimethylether) was applied to the foils to mimic a wax-filled pore. C_{60+} melts above 373 K and, in order to coat the foil, lumps of solidified wax were therefore deposited on both sides of the foil at room temperature in the reactor. Upon heating under syngas the wax melted and formed a liquid layer coating the foil. The thickness of the wax layer was estimated to be of the order of 0.1 mm. Since the C_{60+} wax was applied as solid lumps, which liquefy and spread out over the foil at elevated temperatures in the reactor, the coverage was difficult to control. Therefore a layer of Santovac, which is liquid at room temperature, was also applied. In both cases it was necessary to avoid conditions that cause decomposition of the wax/Santovac. This meant that the Co foil could not be reduced at 573 K once the layer had been applied. For this reason reduced Co foil was "passivated" (i.e., slowly oxidized) at room temperature after catalytic tests by slowly bleeding air into the reactor over several hours. Reduction of the thus passivated Co foils could then be obtained at 493 K under synthesis gas, preventing fast decomposition of the applied layer. The activity and selectivity of the Co foil are not influenced by such a passivation/reduction treatment. It should be noted, however, that under reaction conditions a slow degrading of wax/Santovac took place as was indicated by fragmentation peaks in the chromatograms.

RESULTS

To obtain insight into the chain length dependence of the α-olefin readsorption rate, the influence of several parameters on both the total product concentration and the paraffin/olefin ratio have been measured as a function of carbon number. At first the influence of the H_2/CO ratio has been measured. The H_2/CO ratio was changed while keeping the H_2 flow, the total flow and the pressure constant (1.25 Nml/min, 5 Nml/min, 1 bar) by adding He. A polycrystalline Co foil with a total surface area of 20 cm^2 was used as the catalyst. In Fig. 2a the total product concentration, i.e., the combined concentration of (branched and linear) paraffins and olefins, is plotted for various H_2/CO ratios. Apart from C_1 and C_2 the concentration shows an exponential decrease with carbon number. As might be expected [18], Fig. 2a clearly shows that the chain growth probability, α, decreases with increasing H_2/CO ratio. The CH_4 make increases with H_2/CO. Since the H_2 pressure was kept constant, this implies that the methane concentration decreases with increasing CO pressure in this regime. In Fig. 2b the paraffin/olefin ratio (P_n/O_n) is plotted for the various H_2/CO ratios. P_n/O_n

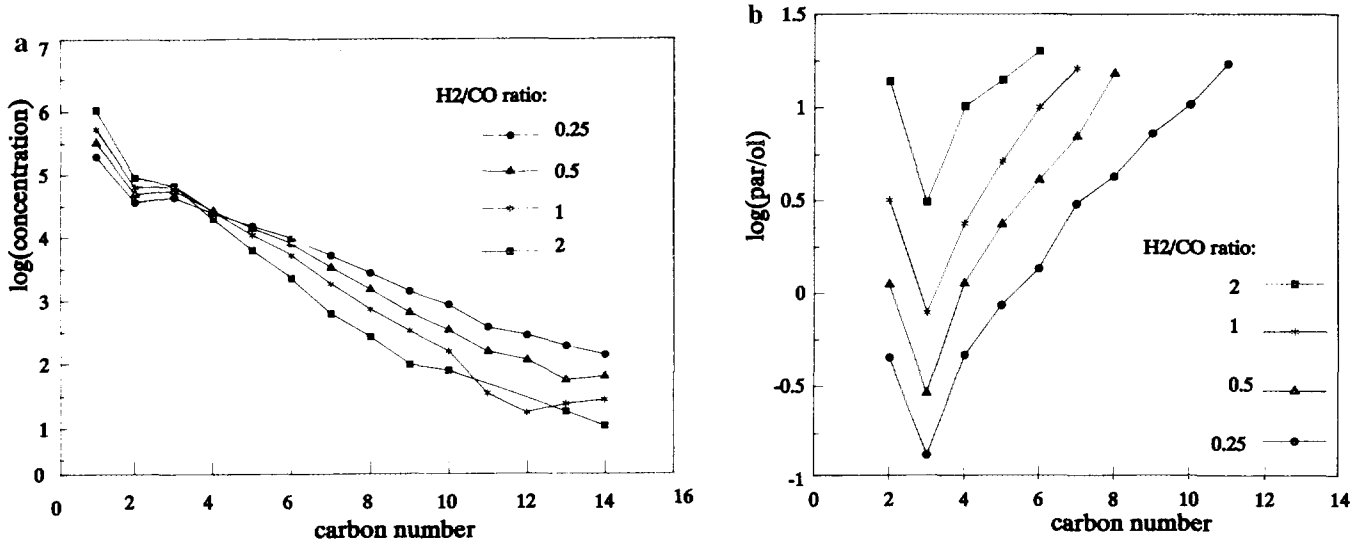

FIG. 2. (a) Total product concentration (ppb) obtained on a 20 cm^2 Co foil (reduced at 573 K for 25 min) as a function of carbon number for various H_2/CO ratios. T = 493 K, total flow = 5 Nml/min, H_2 flow = 1.25 Nml/min, P = 1 bar. (b) Paraffin/olefin ratio as a function of H_2/CO ratio.

increases exponentially with chain length and this chain length dependence is roughly the same for all four H_2/CO ratios used. The paraffin selectivity increases with H_2/CO ratio.

Using a 25 cm^2 foil the effect of the total flow on the overall product concentration and the P_n/O_n ratio has been measured. Results are plotted in Figs. 3a and 3b, respectively. Figure 3a shows that the conversion decreases with increasing flow. Figure 3b shows that the paraffin selectivity decreases with increasing flow.

To obtain information on the effect of "catalyst loading" on the paraffin/olefin ratio, experiments were carried out using various Co foils with different surface areas (25 cm^2, 5.5 cm^2, and 0.55 cm^2). In Figs. 4a and 4b the total product concentration and P_n/O_n are plotted respectively for these different pieces of Co foil. Figure 4a shows product concentrations decreasing with decreasing Co foil surface area. Figure 4b shows a P_n/O_n which decreases when the surface area decreases from 25 to 5.5 cm^2. Note that for the 0.55 cm^2 foil the paraffin signal was too low to be detected.

Since the CO conversion was kept very low (<1%), and the catalytic tests did not last longer than a few hours, no significant wax layer could be formed on the Co foil

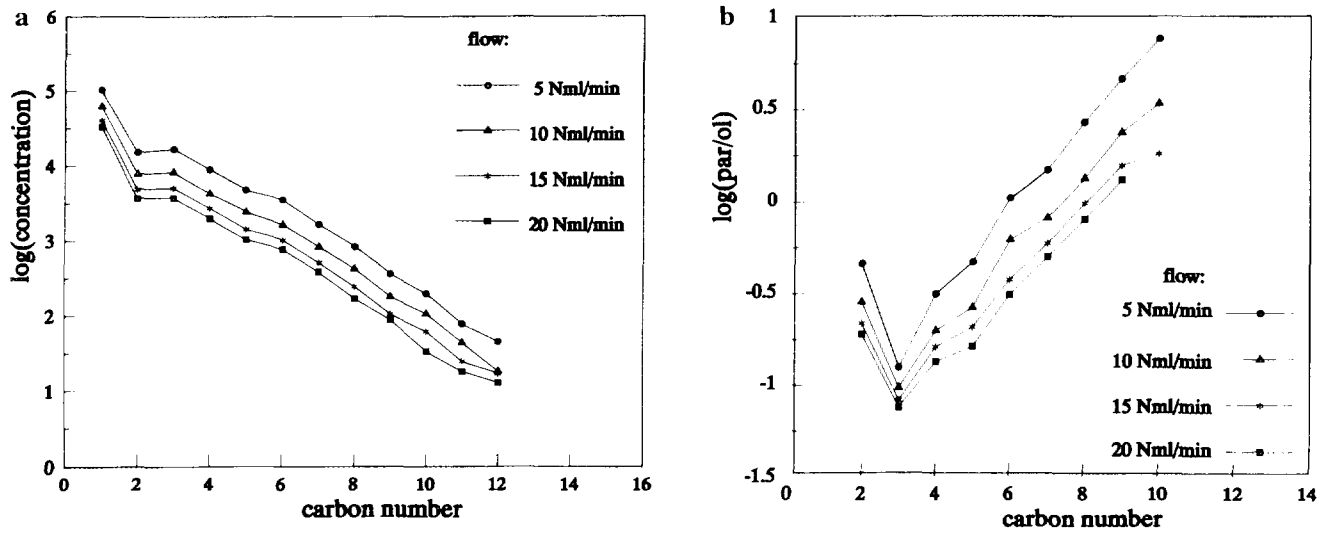

FIG. 3. (a) Total product concentration (ppb) obtained on a 25 cm^2 Co foil (reduced at 573 K for 5 min) as a function of carbon number for various flows. T = 493 K, H_2/CO = 2, P = 1 bar. (b) Paraffin/olefin ratio as a function of the flow.

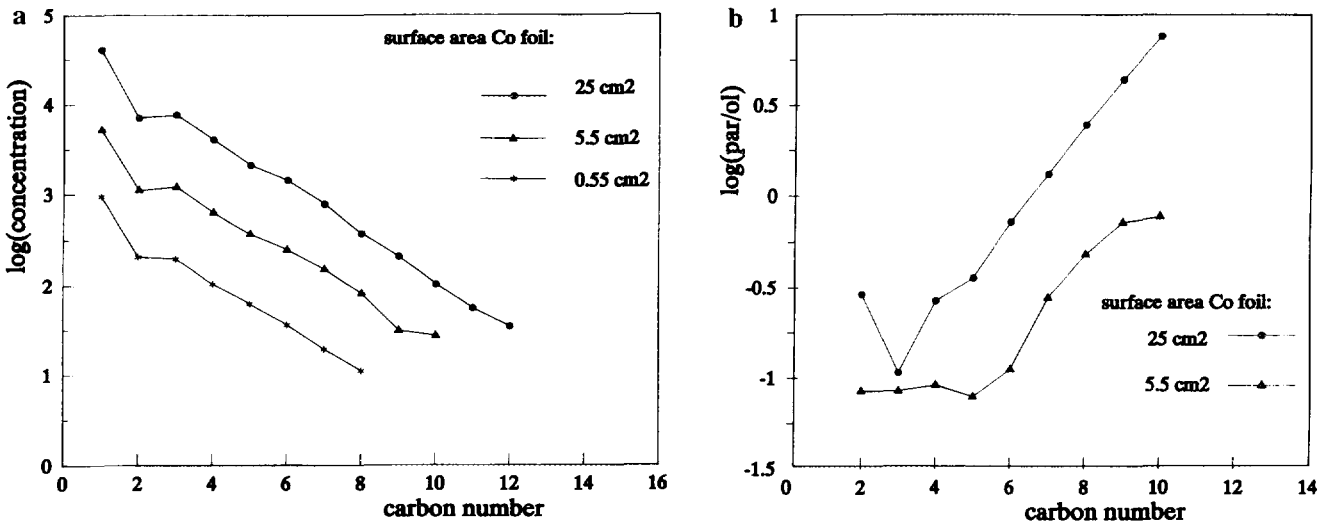

FIG. 4. (a) Total product concentration (ppb) obtained on different Co foils (reduced at 573 K for 5 min) as a function of carbon number for various surface areas. T = 493 K, H_2/CO = 2, P = 1 bar, flow = 5 Nml/min. (b) Paraffin/olefin ratio as a function of the surface area.

during the experiments. Thus the removal of products formed on the Co foil was not hindered by diffusion through a thick layer of wax. However, diffusion limitation could be introduced by coating the foils with a layer of C_{60+} FT wax. The vapour pressure of this wax is too low to cause any detection interference with the C_{15-} formed and detected during the experiments. The influence of the wax layer on both the total product concentration and P_n/O_n is shown in Figs. 5a and 5b, respectively. The total product concentration decreases only slightly, whereas the paraffin selectivity decreases strongly due to the application of a wax layer. Figure 5b clearly shows that the chain length dependence of P_n/O_n becomes much weaker due to the wax layer. The influence of a layer of Santovac oil on both the total product concentration and P_n/O_n is shown in Figs. 6a and 6b, respectively. The product concentration decreases only slightly, whereas the paraffin selectivity decreases strongly due to the application of Santovac. Figures 6a and 6b show that the chain length dependence of P_n/O_n becomes much weaker whereas the chain growth probability increases due to the Santovac layer.

Two additional experiments were made to check whether diffusion limitation is indeed "switched on" by

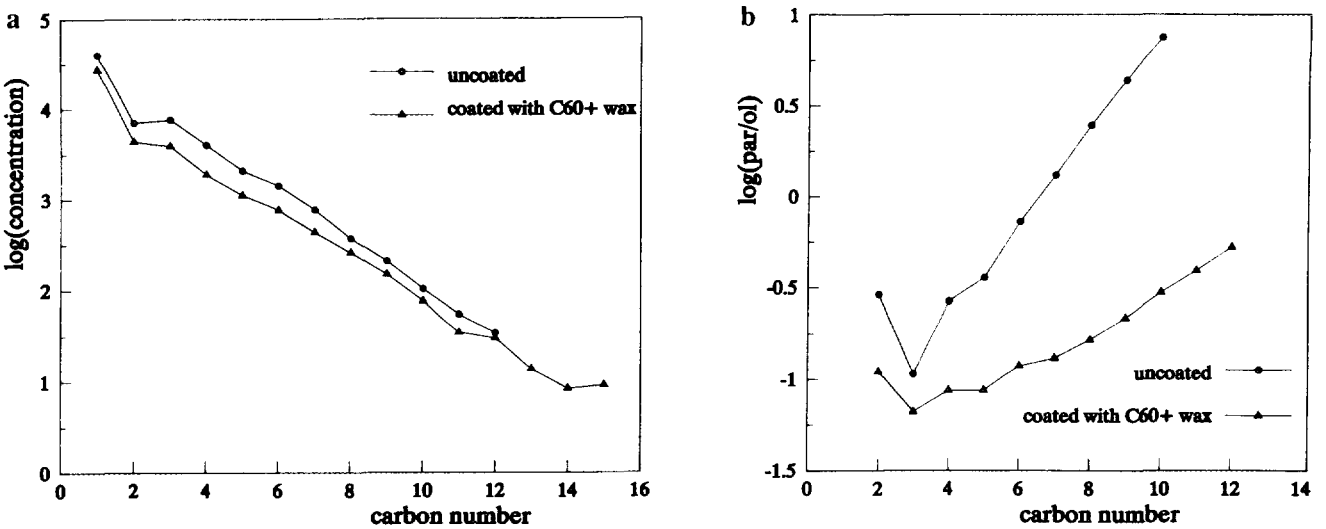

FIG. 5. (a) The effect of a C_{60+}-wax coating on the total product concentration (ppb) of a 25 cm^2 Co foil (reduced at 573 K for 5 min), T = 493 K, H_2/CO = 2, P = 1 bar, flow = 5 N ml/min. (b) The effect of a C_{60+}-wax coating on the paraffin/olefin ratio.

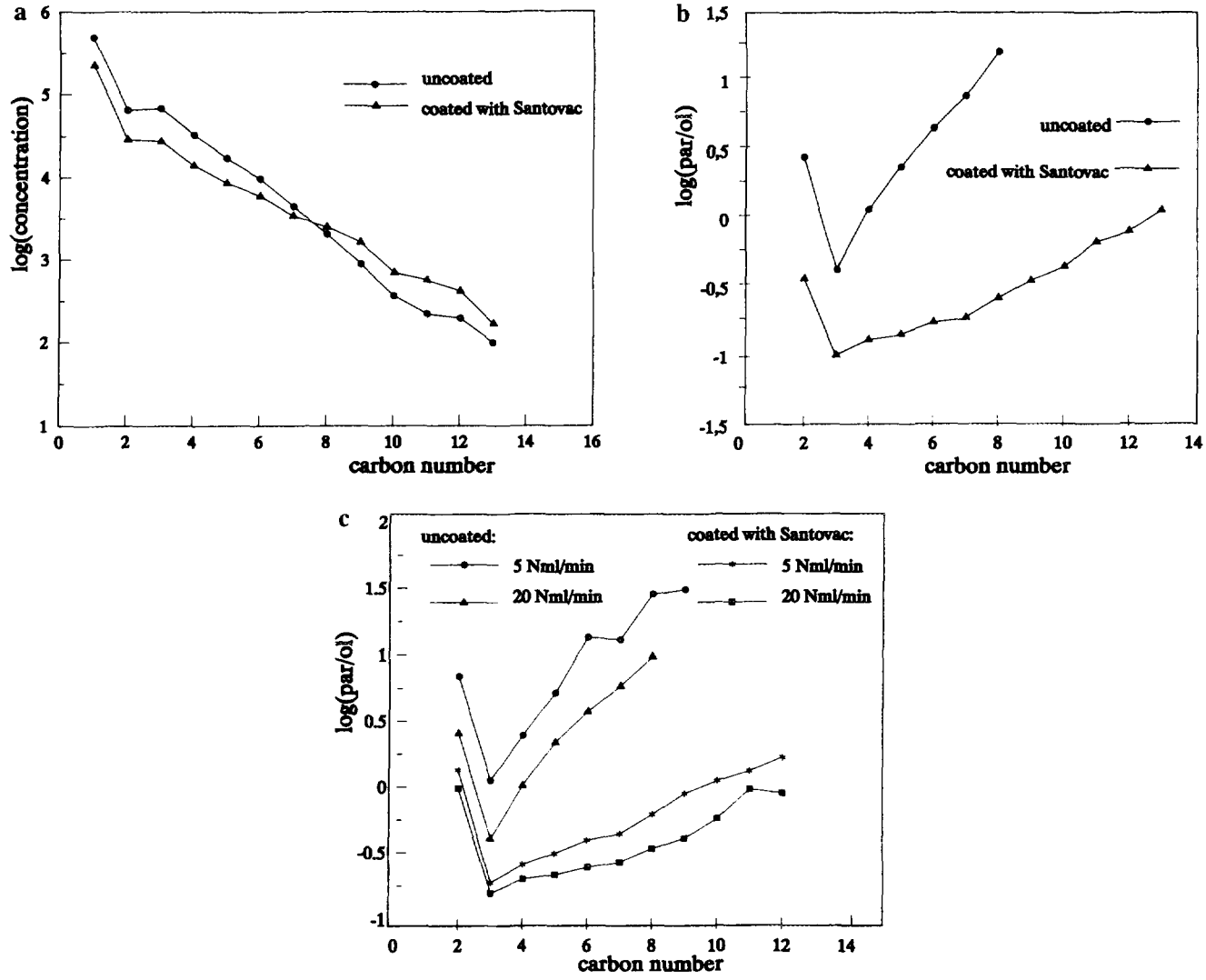

FIG. 6. (a) The effect of a Santovac coating on the total product concentration (ppb) of a 15 cm^2 Co foil (reduced at 573 K for 15 min), T = 493 K, H_2/CO = 2, P = 1 bar, flow = 5 Nml/min. (b) The effect of a Santovac coating on the paraffin/olefin ratio. (c) The effect of the flow on the paraffin/olefin ratio for both an uncoated and a Santovac coated foil.

coating with Santovac. At first the influence of the flow velocity on P_n/O_n was measured for both a coated and an uncoated foil. If P_n/O_n is only caused by transport limitation it will hardly be affected by the flow velocity. Thus the effect of flow velocity on P_n/O_n, shown in Fig. 6c, is a measure of the influence of transport limitation. As a double check the rate of hydrogenation of extra hexene added to the flow has also been measured. The added concentration was around 50 ppm, which is similar to the concentration of hexene produced in the reactor.

For the uncoated Co foil there was no difference in the hydrogenated fraction of the added and the synthesized hexene. For a Santovac-coated foil, however, the hydrogenated fraction of the added hexene was a factor of about three smaller, showing that transport limitation occurs.

DISCUSSION

In the Fischer–Tropsch reaction growing linear alkyl chains are chemically bound to the surface. This latter bond can be broken either by β-hydrogen abstraction yielding an α-olefin, or by α-hydrogenation yielding an n-paraffin. The thus formed n-paraffin is non-reactive under FT conditions and therefore not prone to secondary conversions, whereas the α-olefins are reactive under FT conditions and have a finite probability of being hydrogenated or reinserted into the chain growth reaction by readsorption into the catalyst. Olefin readsorption reverses the termination by dehydrogenation, causing an increase of both the effective chain growth probability and the paraffin/olefin ratio (10).

The probability of a secondary reaction for an α-olefin is believed to increase strongly with carbon number, since both the paraffin/olefin ratio (19, 20) and the growth probability (10, 20) increase with chain length. In the literature two different explanations are given for this chain length dependence. In both explanations the secondary reaction probability is assumed to be proportional to the contact time. Several authors suggest that the contact time strongly increases with chain length due to the greater solubility of longer hydrocarbons in the FT wax inside the pores (14, 20). Since the chain length dependence of the solubility has not been measured or calculated directly, the solubility argument has as yet only been used qualitatively. The solubility is described by the so-called Henry coefficient, which in turn can be found using Raoult's law and the vapour pressures (21) of the pure wax components as calculated with the Clausius–Clapeyron equation (22). The thus found chain length dependence of the solubility in the wax mixture is shown in Fig. 7. The dependence of the solubility on chain length is almost exponential and can be fitted with $e^{(0.55\pm0.10)n}$ in which n is the carbon number. A similar chain length dependence is found for the paraffin/olefin ratio in Figs. 2b, 3b, and 4b. Nevertheless Iglesia *et al.* have rejected the solubility argument, stating that the presence of a liquid phase does not affect the chemical potentials and thus has no effect on secondary reactions (10). They suggest that transport limitations cause a chain-length-dependent contact time, since the results of various contact time and co-feeding studies could be fitted using an analytical model in which a chain-length-dependent intraparticle diffusion coefficient for olefins through FT wax had been incorporated [10–13]. The diffusion coefficient, D_n ($m^2 \cdot s^{-1}$), which was used by Iglesia *et al.* for fitting their data, decreases with carbon number n as (10):

$$D_n = D_0 \cdot e^{-0.3n}. \qquad [1]$$

This dependence has not been confirmed by a direct measurement of the diffusion coefficient or by comparison with the diffusion coefficients of n–C_8H_{18}, n–$C_{12}H_{26}$ and n–$C_{16}H_{34}$ through FT wax which have been reported in the literature (23). The carbon number dependence of these measured diffusion coefficients is a factor of five weaker than the one used by Iglesia *et al.* Furthermore polymer dynamics predicts a dependence proportional to $n^{-0.6}$ rather than the exponential dependence given in Eq. [1] (24). Thus it seems improbable that the observed exponential chain length dependence is merely due to diffusion.

We have tried to obtain more insight into the origin of the chain length dependence of the secondary reaction rate by using polycrystalline Co foils as model catalysts. Diffusion limitation can then be completely "switched off" by testing on uncoated Co foils, and can be "switched on" by application of a wax/Santovac layer to the Co foils. The disadvantage of model catalysts is their very low surface area, producing only a small concentration of hydrocarbons of which the concentration up to around C_{14} could be determined, as can be seen in Figs. 2a, 3a, 4a, 5a, and 6a.

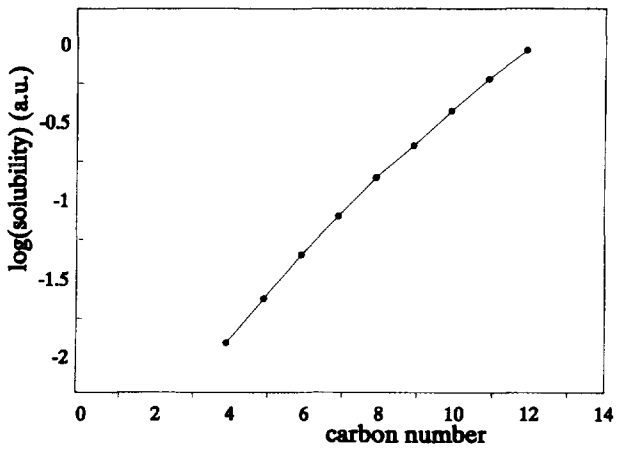

FIG. 7. Chain length dependence of the solubility calculated using Raoult's law (solubility $\propto 1/C^s_{n\,vap}$) and the Clausius-Clapeyron equation.

Readsorbed olefins can either be hydrogenated or reinserted. The ratio of hydrogenation over reinsertion depends on many parameters such as the partial pressures of CO and H_2O (10). Under the experimental conditions used, practically all readsorbed olefins will be hydrogenated. Thus, at least up to C_{14} the product distribution does not deviate from an ASF distribution, so the role of secondary reactions cannot be deduced from an ASF-distribution deviation. The chemisorbed intermediate which leads to hydrogenation differs from the intermediate which leads to reinsertion/chain growth (25). However, the chain length dependence of both hydrogenation and reinsertion will be governed by the same factors. Thus to obtain information on the chain length dependence of secondary reactions the chain length dependence of the paraffin/olefin ratio (P_n/O_n) can be monitored instead. As can be seen in Figs. 2b, 3b, 4b, 5b and 6b, P_n/O_n increases exponentially with carbon number. Thus the rate of readsorption of an α-olefin increases exponentially with chain length. In the case of uncoated Co foils, this chain length dependence can be fitted by

$$\frac{P_n}{O_n} = R_0 \cdot e^{cn} \qquad [2]$$

in which $c = 0.55 \pm 0.05$, and R_0 is a constant. Comparable carbon number dependences can be deduced for the case of porous catalysts, e.g., Konig and Gaube (5). The paraf-

fin/olefin ratio found by Iglesia *et al.* for high CO conversion also shows a strong exponential dependence which could be fitted by us with $c = 0.45$.[1]

Although the dependence observed in the above described experiments on uncoated foils is similar to that observed for porous catalysts at high conversions, it is certain that diffusion limitations are completely absent. To explain the results obtained we propose the following model which basically uses the concentration of hydrocarbons in the physisorbed layer over the surface as the crucial factor rather than the "reactor hold-up" used by others.

For reinsertion, an olefin has to chemisorb at a vacant site at the surface of the catalyst. Under FT conditions such a vacant site is rare, since the surface is almost completely covered with a variety of species (26). Once a "chain-growth site" becomes vacant, an olefin has to compete with CO and H_2 for its occupation. It is very unlikely that an olefin far removed from the vacant site will reach the site before it has been occupied again. Thus of all the olefins inside the reactor only those in the near neighbourhood have a chance of readsorption and therefore the reinsertion rate should be coupled to the olefin concentration at the interface in the physisorbed layer (or precursor state) instead of to the reactor-averaged concentration (i.e., contact time). Besides transport limitation, preferential physisorption and solubility will have a strong influence on the interface concentration and should thus be taken into account for describing the readsorption rate. As they are naturally in equilibrium, these last two terms do not change the chemical potentials and thus this might seem inappropriate (10). However, as described above, the chemisorption of an olefin is a non-activated process. Competition for reaction does only take place in the transfer from the precursor state (physisorption) to the chemisorbed state. Thus the readsorption rate is only controlled by the effective "collision rate," which is governed by the concentration in the physisorbed interface, i.e. a resultant of contact time in the physisorbed interface and the concentration in the wax. To put it briefly: although the chemisorbed phase is a steady state, there is no equilibrium between the physisorbed and the chemisorbed phase.

To derive an expression for the olefin concentration at the physisorbed interface we will make use of the schematic diagram of a wax-coated catalyst shown in Fig. 8. Assuming that all products leave the reactor in the vapour phase, the vapour phase concentration of an olefin with chain length n, $C^{=}_{n\,\mathrm{vap}}$ (m^{-3}), can be given by

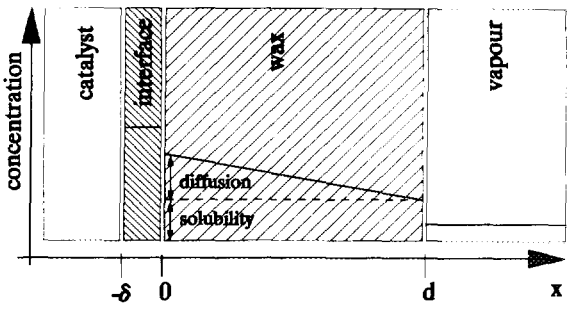

FIG. 8. Schematic representation of the olefin concentration profile on a wax/Santovac coated catalyst.

$$C^{=}_{n\,\mathrm{vap}} = \frac{O^{\mathrm{net}}_{n} \cdot A}{\Phi} \qquad [3]$$

in which A is the surface area of the catalyst (m^2), O^{net}_{n} is the amount of α-olefins with chain length n which are effectively produced (i.e., after subtraction of olefins which are hydrogenated or reinserted by secondary reactions) per m^2 of catalyst per second ($\mathrm{m}^{-2} \cdot \mathrm{s}^{-1}$) and Φ is the flow ($\mathrm{m}^3 \cdot \mathrm{s}^{-1}$). At their interface ($x = d$) wax and vapour are in equilibrium and thus the concentration of olefins with chain length n dissolved in the wax, $C^{=}_{n\,\mathrm{wax}}$ ($x = d$) (m^{-3}), is given by Raoult's law (27).

$$C^{=}_{n\,\mathrm{wax}}(x = d) = \frac{C^{=}_{n\,\mathrm{vap}}}{C^{\mathrm{s}}_{n\,\mathrm{vap}} \cdot V^{\mathrm{m}}_{n\,\mathrm{wax}}} = \frac{O^{\mathrm{net}}_{n} \cdot \mathrm{A}}{\Phi \cdot C^{\mathrm{s}}_{n\,\mathrm{vap}} \cdot V^{\mathrm{m}}_{n\,\mathrm{wax}}} \qquad [4]$$

in which $V^{\mathrm{m}}_{n\,\mathrm{wax}}$ (m^3) is the molar volume of wax consisting solely of hydrocarbons with chain length n and $C^{\mathrm{s}}_{n\,\mathrm{vap}}$ (m^{-3}) is its saturated vapour phase concentration. In case of an equilibrium there would be no concentration gradient through the wax layer, so $C_{n\,\mathrm{wax}}$ ($x = 0$) would equal $C_{n\,\mathrm{wax}}$ ($x = d$). However, there is a net production of hydrocarbons (a steady state rather than an equilibrium), and thus for their drainage there has to be a concentration gradient over the layer, $\Delta C^{=}_{n\,\mathrm{diff}}$ (m^{-3}):

$$\Delta C^{=}_{n\,\mathrm{diff}} = \frac{O^{\mathrm{net}}_{n} \cdot d}{D_n}. \qquad [5]$$

Combining [4] and [5] gives the concentration close to the liquid-to-solid interface:

[1] Note that this dependence is much stronger than the $n^{1/2}$ dependence (short chains) or the $e^{0.3 \cdot n}$ (long chains) predicted by their own model. In a later publication it was suggested that this discrepancy might be caused by the expected increase in the severity of transport restrictions as thicker liquid layers between catalyst pellets are formed at low linear gas velocities (i.e., high conversions) (13). However, implementation of this scenario into their model can fundamentally still not explain a chain length dependence stronger than $e^{0.3 \cdot n}$ and would also predict a further increase in the rate of secondary reactions, which for low carbon numbers was already found to be too high (10, 13).

$$C^{=}_{n\,\mathrm{wax}}(x=0) = C^{=}_{n\,\mathrm{wax}}(x=d) + \Delta C^{=}_{n\,\mathrm{diff}} = \frac{O^{\mathrm{net}}_n \cdot A}{\Phi \cdot C^{\mathrm{s}}_{n\,\mathrm{vap}} \cdot V^{\mathrm{m}}_{n\,\mathrm{wax}}} + \frac{O^{\mathrm{net}}_n \cdot d}{D_n}. \quad [6]$$

This equation holds for the concentration inside the wax layer. At the liquid-to-solid interface ($x = -\delta$), however, preferential physisorption will occur. A hydrocarbon is physisorbed more strongly at the Co foil than dissolved in the wax, which is manifested in the total wetting of metals by hydrocarbons (28) and in the heat generated by the immersion of metals in hydrocarbons (29). Physisorption is governed by Van der Waals attraction and the physisorption energy will depend almost linearly on chain length for hydrocarbons that are not too long (30–32) and is expected to level off only at very high values. Therefore $\Delta G_{n\,\mathrm{phys}}$, the change of free energy for the physisorption of a hydrocarbon with chain length n out of the wax onto the solid-to-wax interface, can be approximated by $n \cdot \Delta G_{1\,\mathrm{phys}}$, and so the contact time at the solid-to-liquid interface will increase exponentially with chain length, which effects an enrichment at the interface of the longest chains in case of a hydrocarbon mixture (33, 34). After correction for this effect the following form is obtained for $X^{=}_{n\,\mathrm{wax}}(x = -\delta)$, the fraction of the liquid-to-solid interface ($x = -\delta$ in Fig. 8) occupied by olefins with chain length n

$$X^{=}_{n\,\mathrm{wax}}(x=-\delta) = n \cdot k_0 \cdot C^{=}_{n\,\mathrm{wax}}(x=0) \cdot \frac{e^{n\cdot\Delta G_{1\,\mathrm{phys}}/RT}}{1 + \sum_{n\to\infty}(n \cdot k_0 \cdot (C^{=}_{n\,\mathrm{wax}}(x=0) + C_{n\,\mathrm{wax}}(x=0)) \cdot e^{n\cdot\Delta G_{1\,\mathrm{phys}}/RT}) + C_{\mathrm{Co}} + C_{\mathrm{H_2}}} \quad [7]$$

in which k_0 is a constant (m^3) and $C_{n\,\mathrm{wax}}(x = 0)$ (m^{-3}) is the concentration of paraffins with chain length n dissolved in the wax. (Note that in Eq. [7] only competitive physisorption—i.e., physisorption as opposed to chemisorption—of hydrocarbons is taken into account). Recently Komaya and Bell also introduced a physisorbed state in their model for FT synthesis (36). They concluded that the holdup of hydrocarbons in a weakly physisorbed state was significant for readsorption of C_{6+} products on a Ru/TiO_2 catalyst. In our model the readsorption rate of olefins is directly proportional to $X^{=}_{n\,\mathrm{wax}}(x = -\delta)/n$. The amount of paraffins with carbon number n effectively produced (i.e., primary + secondary paraffins), P^{net}_n, ($m^{-2} \cdot s^{-1}$), can be given by

$$P^{\mathrm{net}}_n = \frac{k_1}{n} \cdot X^{=}_{n\,\mathrm{wax}}(x=-\delta) + P^{\mathrm{prim}}_n \quad [8]$$

in which k_1 is a constant ($m^{-2} \cdot s^{-1}$) and P^{prim}_n is the amount of primary paraffins produced ($m^{-2} \cdot s^{-1}$). Since the hydrogenation/dehydrogenation rate of growing chains is n-independent

$$P^{\mathrm{prim}}_n = k_2 \cdot O^{\mathrm{prim}}_n = k_2 \left(O^{\mathrm{net}}_n + \frac{k_3}{n} \cdot X^{=}_{n\,\mathrm{wax}}(x=-\delta) \right) \quad [9]$$

in which k_2 and k_3 are constants, O^{prim}_n is the amount of primary α-olefins produced ($m^{-2} \cdot s^{-1}$). (Note, that $k_1 \neq k_3$ since k_1 only covers the hydrogenated fraction of the readsorbed olefins, whereas k_3 covers the reinserted fraction as well). Combining eqs. [7, 8, and 9] yields the following expression for P_n/O_n:

$$\frac{P_n}{O_n} = \frac{P^{\mathrm{net}}_n}{O^{\mathrm{net}}_n} = k_0 \cdot (k_1 + k_2 \cdot k_3) \cdot \left[\frac{A}{\Phi \cdot C^{\mathrm{s}}_{n\,\mathrm{vap}} \cdot V^{\mathrm{m}}_{n\,\mathrm{wax}}} + \frac{d}{D_n} \right] \cdot \frac{e^{n\Delta G_{1\,\mathrm{phys}}/RT}}{1 + \sum_{n\to\infty}(n \cdot k_0 \cdot (C^{=}_{n\,\mathrm{wax}}(x=0) + C_{n\,\mathrm{wax}}(x=0)) \cdot e^{n\Delta G_{1\,\mathrm{phys}}/RT}) + C_{\mathrm{Co}} + C_{\mathrm{H_2}}} + k_2. \quad [10]$$

Equation [10] shows that P_n/O_n contains an equilibrium term (i.e., physisorption in equilibrium with the vapour phase) and a transport limitation term. The n-dependence of the equilibrium term originates from the n-dependence of both physisorption and solubility, whereas the n-dependence of the transport limitation term originates from the n-dependence of both physisorption and diffusion.

For the case of a bare foil, d will be near zero and hence the equilibrium term will dominate the transport limitation term. Thus the chain length dependence is governed by

$(C^s_{n\,vap} \cdot V^m_{n\,wax})^{-1}$ corrected for the preferential adsorption of wax molecules on the foil-to-wax interface, $e^{n\Delta G_{1\,phys}/RT}$. In Fig. 7 it is shown that $1/C^s_{n\,vap}$ (i.e., solubility) increases almost exponentially with n. As mentioned previously, $1/C^s_{n\,vap} \propto e^{(0.55\pm0.10)n}$. An almost linear increase with n is expected for $V^m_{n\,wax}$ (35), and the preferential adsorption increases exponentially with n. Thus it is expected that $P_n/O_n \propto (1/n)\ \exp\{(\Delta G_{1\,phys}/RT + 0.55)n\}$. If this expression is fitted to the data obtained for P_n/O_n on a bare foil, we find that $\Delta G_{1\,phys}/RT = 0.2 \pm 0.1$. (Note that the exponential n-dependence is much stronger than the reciprocal one, which explains the experimentally observed and previously mentioned exponential chain length dependence, $c = 0.55 \pm 0.05$). Equation [10] shows that for the case of a negligible diffusion limitation the readsorption rate should decrease linearly with increasing Φ and decreasing surface area, A, which was observed in the case of the uncoated foil as shown in Figs. 3b and 4b, respectively. As shown earlier, the α-olefins have to compete with CO for the occupation of a vacant site, causing the readsorption rates (k_1, k_3) to decrease with increasing CO-pressure, which is indeed observed experimentally as shown in Fig. 2b.

Equation [10] shows that the influence of the transport limitation becomes dominant in the case of a thick coating and for small values of A/Φ (i.e., small contact times, low conversions). For all experiments the conversions were so low that the transport limitation can dominate the equilibrium term already for a submillimeter wax layer. The role of transport limitation is independent of Φ, whereas the influence of the equilibrium term decreases linearly with Φ. So the Φ-dependence of P_n/O_n contains information on the role of transport limitation. As shown in Fig. 6c, a four-fold increase of Φ results in an almost four-fold decrease of P_n/O_n for the case of a bare foil (exactly four-fold is only expected in the case of negligible production of primary paraffins, i.e., $k_2 = 0$). For a coated foil this decrease is much less for the shorter chain indicating the occurrence of transport limitation. From Fig. 6c it can be deduced that in the case of hexene around $\frac{2}{3}$ of the hydrogenation is caused by transport limitation. The same number is also obtained from the hydrogenated fraction of hexene purposely added to the feed, since for the case of a coated foil this fraction was a factor of about three lower than for the synthesized hexene. Thus, since up to $n = 6$ the major part of the hydrogenation is governed by transport limitation, the exponential dependence of $1/C^s_{n\,vap}$ is no longer included. Therefore the chain length dependence will become weaker with a proper coating, which is indeed observed as shown in Figs. 5b and 6b. The following relation between the paraffin/olefin ratio and carbon number is expected:

$$P_n/O_n \propto e^{n\Delta G_{1\,phys}/RT}/D_n \propto e^{(0.2\pm0.1)\cdot n} \cdot n^{0.6}.$$

The data in Figs. 5b and 6b can indeed be fitted with this dependence. A decrease of the chain length dependence, however, is not the only effect of the coating. The same figures also clearly show that the net readsorption rate decreases considerably. In the case of diffusion limitation one would expect an increase, since it becomes more difficult for the primary products to escape. The decrease can be understood by the preferential physisorption of longer hydrocarbons. In case of a wax/Santovac coating the just produced olefins will be "pushed" away from the interface by the much longer, i.e. more strongly physisorbed, C_{60+}/Santovac. In Eq. [10] the denominator, $\Sigma_{n\to\infty}\,(n \cdot k_0 \cdot (c^{=}_{n\,wax}\,(x = 0) + c_{n\,wax}\,(x = 0)) \cdot e^{n\Delta G_{1\,phys}})$, will become much larger since the sum will now also include many strongly adsorbed C_{60+}/Santovac molecules.

From the above it can be concluded that for a flat model catalyst the chain length dependence of the paraffin/olefin ratio is either ruled by equilibrium (i.e. physisorption in equilibrium with vapour) or by transport limitation. In both cases P_n/O_n increases exponentially with chain length. In the case of transport limitation this exponential dependence is rather weak and is caused by a preferential physisorption of the longer chains at the catalyst-to-wax interface and hardly by the n-dependence of the diffusion coefficient itself. In the absence of transport limitations, solubility will rule the concentration and thus, due to the Henry coefficient, a stronger exponential n-dependence will be observed. Transport limitation increases with the thickness of the wax layer, whereas the role of the solubility increases with the partial pressure of the olefins in the reactor. Thus for an experiment with a Co foil, transport limitation can only dominate solubility at low conversions and long diffusion paths. Even then transport limitation will, counterintuitively, only occur for short chains, since the role of solubility increases much more strongly with chain length. In Fig. 9 this is shown schematically. The model presented above can be qualitatively applied to porous catalysts as well. For a quantitative approach (especially of the transport limitation (10)) many more parameters which characterise the catalyst have to be taken into account. However, even if transport limitation occurs, it will only be dominant for short chains (14). Note that in the above described experiments/model all the products leave the reactor in the vapour phase. If products were to leave the reactor as a liquid the solubility should not be taken into account. In that case the carbon number dependence would only be caused by transport limitation and preferential physisorption.

CONCLUSIONS

Low conversion FT synthesis on Co foil shows a paraffin/olefin ratio increasing exponentially with chain length. Coating the foil with wax/Santovac results in a lower

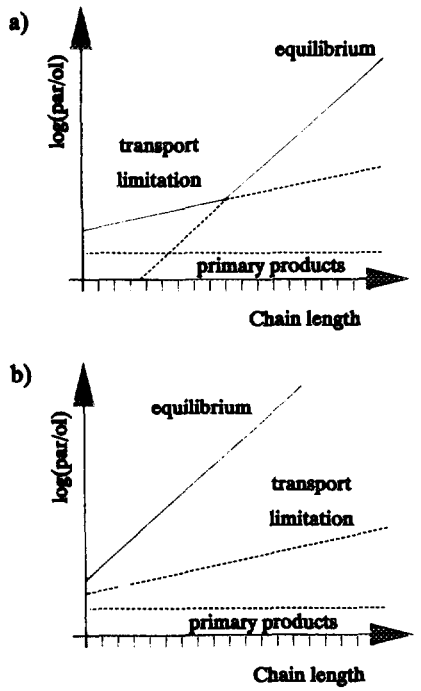

FIG. 9. Schematic representation of the paraffin/olefin ratio for the case of (a) dominant transport limitation and (b) negligible transport limitation.

paraffin production and a weaker chain-length-dependence. These results can be explained by an olefin readsorption rate that increases exponentially with chain length. A model is presented in which the olefins have to compete for readsorption, yielding a readsorption rate proportional to the olefin concentration at the catalyst-to-wax interface. Thus the chain length dependence is caused by solubility and diffusion limitation, both corrected for preferential physisorption at the interface. Under commercial operation, i.e., high CO-conversions, transport limitation will only dominate over solubility under special circumstances.

REFERENCES

1. Maxwell, I. E., and Naber, J. E., *Catal. Lett.* **12,** 105 (1992).
2. Henrici-Olivé, G., and Olivé, S., *Angew. Chem. Int. Ed. Engl.* **15,** 136 (1975).
3. Satterfield, C. N., "Heterogeneous Catalysis in Practice," 2nd ed, p. 432. McGraw–Hill, New York, 1991.
4. Satterfield, C. N., and Huff, G. A., *J. Catal.* **73,** 187 (1982).
5. König, L., and Gaube, J., *Chem. Ing. Tech.* **55,** 14 (1983).
6. Huff, G. A., and Satterfield, C. N., *J. Catal.* **85,** 370 (1984).
7. Egiebor, N. O., Cooper, W. C., and Wojciechowski, B. W., *Can. J. Chem. Eng.* **63,** 826 (1985).
8. Herington, E. F., *Chem. Ind.* **65,** 346 (1946).
9. Novak, S., Madon, R. J., and Suhl, H., *J. Catal.* **77,** 141 (1982).
10. Iglesia, E., Reyes, S. C., and Madon, R. J., *J. Catal.* **129,** 238 (1991).
11. Madon, R. J., Reyes, S. C., and Iglesia, E., *J. Phys. Chem.* **95,** 7795 (1991).
12. Madon, R. J., and Iglesia, E., J. Catal. **139,** 576 (1993).
13. Iglesia, E., Reyes, S. C., Madon, R. J., and Soled, S. L., *Adv. Catal.* **39,** 221 (1993).
14. Tau, L. M., Dabbagh, H. A., and Davis, B. H., *Energy Fuels* **4,** 94 (1990).
15. Schulz, H., Beck, K., and Erich, E., *in* "Studies in Surface Science and Catalysis," (D. M. Bibby, C. D. Chang, R. F. Howe, and S. Yurchak, Eds.), Vol. 36, p. 457, Elsevier, Amsterdam, 1988.
16. Lahtinen, J., Anraku, T., and Somorjai, G. A., *J. Catal.* **142,** 206 (1993).
17. Geerlings, J. J. C., Zonnevylle, M. C., and de Groot, C. P. M., *Surf. Sci.* **241,** 315 (1991).
18. Anderson, R. B., in "The Fischer-Tropsch Synthesis," p. 198. Academic Press, Orlando, 1984.
19. Pichler, H., Schulz, H., and Hojabri, F., *Brennst. Chem.* **44,** 5 (1963).
20. Pichler, H., Schulz, H., and Elstner, M., *Brennst. Chem.* **48,** 78 (1967).
21. "Handbook of Chemistry and Physics," 71st ed., Sect. 6, CRC Press, Boston, 1990.
22. Atkins, P. W., *in* "Physical Chemistry," 4th ed., pp. 143 and 162. Oxford Univ. Press, Oxford, 1990.
23. Erkey, C., Rodden, J. B., and Akgerman, A., *Energy Fuels* **4,** 275 (1990).
24. Doi, M., and Edwards, S. F., *in* "The Theory of Polymer Dynamics" (J. Birman, S. F. Edwards, C. H. Llewellyn Smith, and M. Rees, Eds.), Int. Series of Monographs on Physics, Vol. 73, pp. 91–108. Clarendon Press, Oxford, 1986.
25. Schulz, H., van Steen, E., and Claeys, M., *Catal. Lett.* to appear.
26. Mims, C. A., and McCandlish, L. E., *J. Phys. Chem.* **91,** 929 (1987).
27. Atkins, P. W., *in* "Physical Chemistry," 4th ed. p. 162. Oxford Univ. Press, Oxford, 1990.
28. Zisman, W., *in* "Contact Angle, Wettability and Adhesion" (F. M. Fowkes, Ed.), Advances in Chemistry Series, Vol. 43. American Chemical Society, Washington, D.C., 1964.
29. Zettlemoyer, A. C., *Ind. Eng. Chem.* **57,** 27 (1965).
30. Zhang, R., and Gellman, A. J., *J. Phys. Chem.* **95,** 7433 (1991).
31. Dai, Q., and Gellman, A. J., *J. Phys. Chem.* **95,** 9443 (1991).
32. Dai, Q., and Gellman, A. J., *J. Phys. Chem.* **97,** 10783 (1993).
33. Frisch, H. L., Hellman, M. Y., and Lundberg, J. L., *J. Polym. Sci.* **38,** 441 (1959).
34. Xia, T. K., and Landman, U., *Science* **261,** 1310 (1993).
35. "Handbook of Chemistry and Physics," 71st ed. Sect. 3. CRC Press, Boston, 1990.
36. Komaya, T., and Bell, A. T., *J. Catal.* **146,** 237 (1994).